Dynamic compliance of a deeply buried anchor rod

R.Y.S.Pak
University of Colorado, Boulder, USA

ABSTRACT: A deeply buried anchor rod under the action of a time-harmonic lateral force is under investigation. On modelling the embedding full-space as an elastic medium and the anchor as a one-dimensional structure, the problem is formulated as a Fredholm integral equation of the second kind. Selected results are presented to illustrate the primary characteristics of the system compliance.

1 INTRODUCTION

This investigation is concerned with the determination of the dynamic compliance of a deeply buried anchor rod of finite length under the action of a dynamic lateral force acting at the mid-segment. The problem is of some relevance to the seismic design of soil and rock anchors, soil-structure interaction analysis of lineal buried structures such as tunnels and pipelines, as well as the dynamic performance of a variety of structural and nonstructural components in buildings during earthquakes. It also serves well as a pilot study to the more complicated, but closely-related, problem of a pile under dynamic lateral excitations.

2 PROBLEM STATEMENT

The problem under investigation is depicted in Figure 1. A rod of length L and radius a is fully embedded in an infinite space. A time-harmonic lateral force F_0 of frequency ω is exerted on the anchor at its mid-segment. On adoption of the approach employed by Muki and Sternberg (1969) for a class of load-transfer problems, the present problem can be reduced to the analysis of an extended full-space S and its fictitious reinforcement B_* in the rod region D (see Figure 2). The reinforcement B_* is chosen such that the flexural and inertial properties of region D is the same as the actual rod B. To this end, B_* is assigned a Young's modulus of $E_* = E_r - E_s$ and a mass density of $\rho_* = \rho_r - \rho_s$, where the subscripts r and s denote the corresponding quantities of the rod

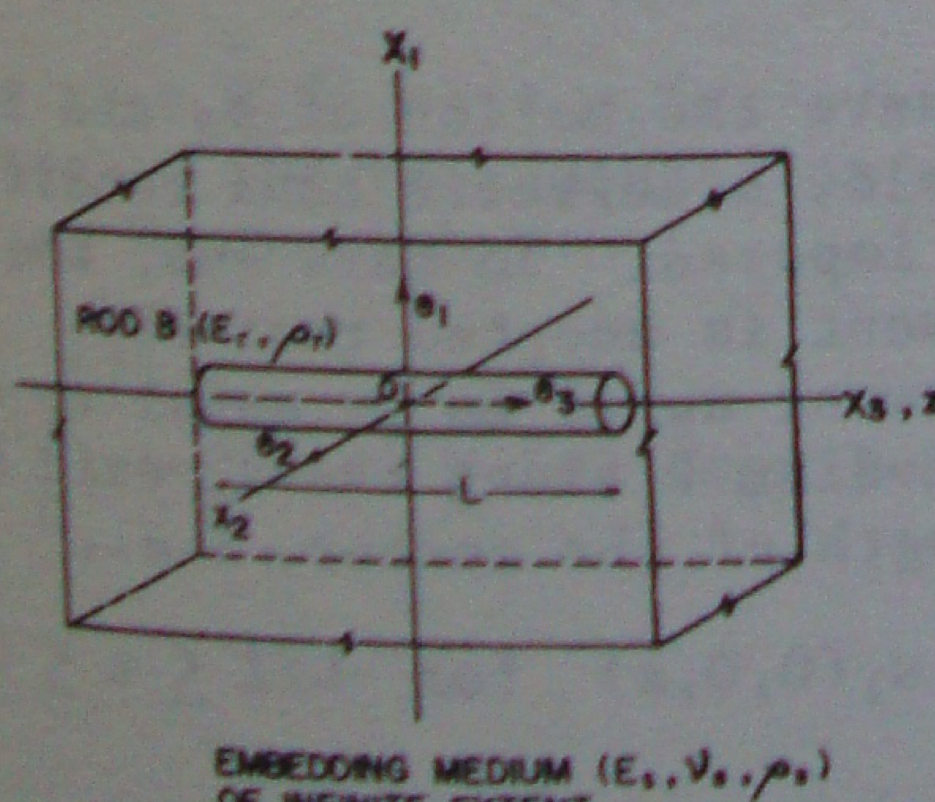

Figure 1: Problem Configuration

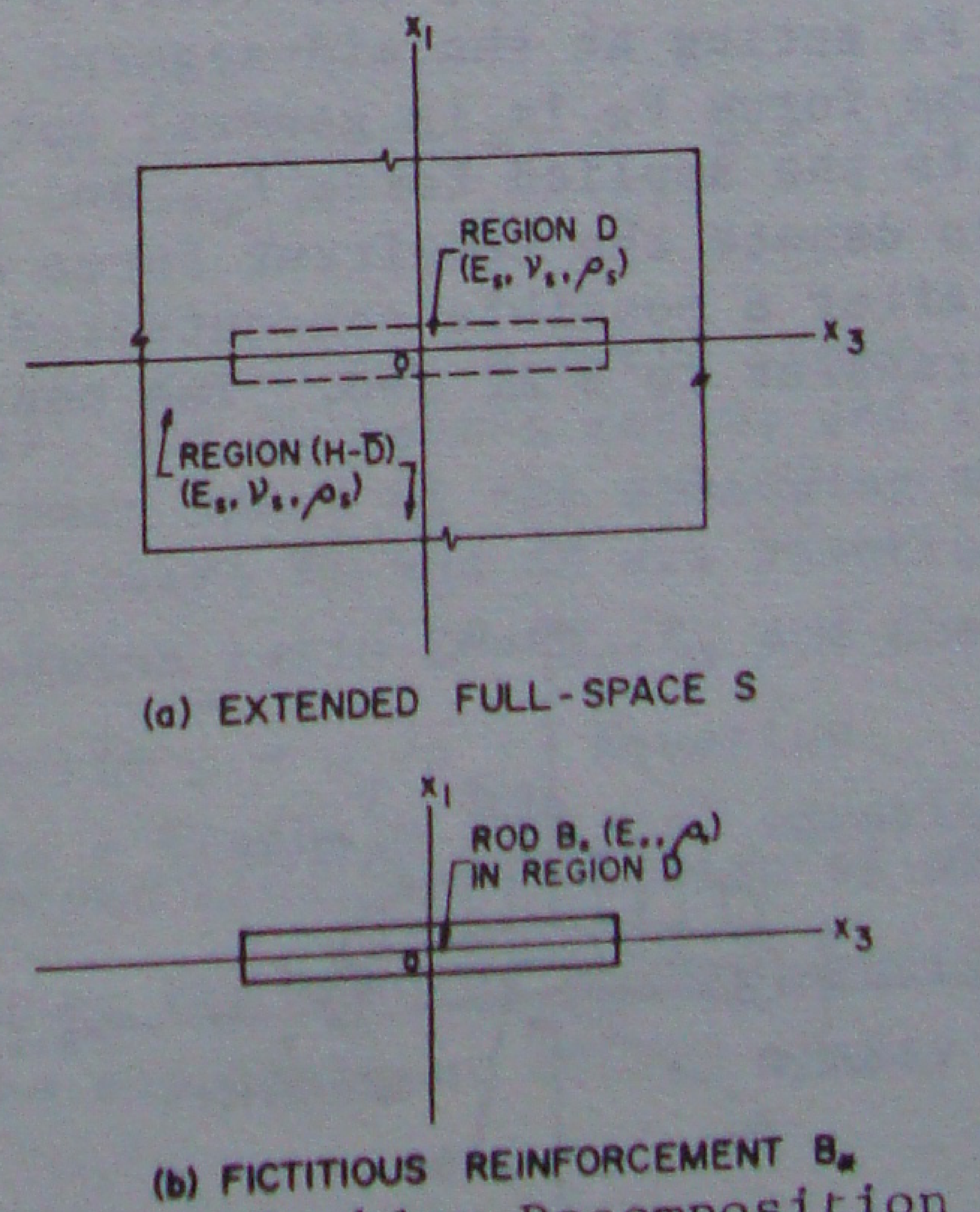

Figure 2: Problem Decomposition

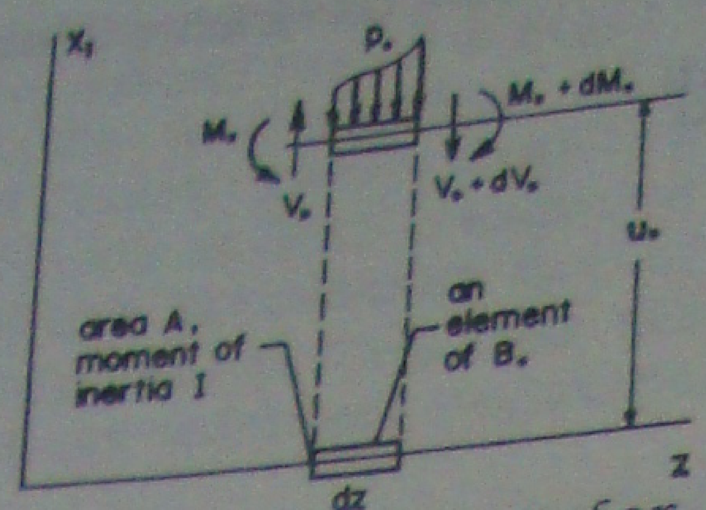

Figure 3: Beam Theory for B_*

and the embedding medium, respectively. Since flexure is primary mode of deformation under the specified loading, B_* is assumed to obey the Bernoulli-Euler beam theory as a first approximation. Accordingly, with the time factor $\{e^{i\omega t}\}$ suppressed from hereon for brevity, the governing equations for B_* are

$$E_* I \frac{d^2 u_*}{dz^2} = -M_* \quad , \qquad (1)$$

$$\frac{dM_*}{dz} = -V_* \quad , \qquad (2)$$

$$p_* = -\frac{dV_*}{dz} + \omega^2 \rho_* A\, u_* \quad , \qquad (3)$$

where the notation and sign conventions are shown in Figure 3. Since the motion of B_* depends on the external forces it is subjected to, it is appropriate at this point to first clarify the interaction forces that are considered in effect between B_* and the extended medium. To this end, the forces that are acting on B_* are shown in Figure 4. They consist of (i) a distributed bond force $p_*(z)$ per unit length acting on the shaft of B_* (ii) the end shear force V_* at $z = \pm L/2$, and (iii) a force F_* acting at the mid-segment of B_*. The force F_* is in general not equal to the applied force F_0, and is used to denote the resultant force acting on B_* after a possible concentrated load-transfer to S at z=0. The need to

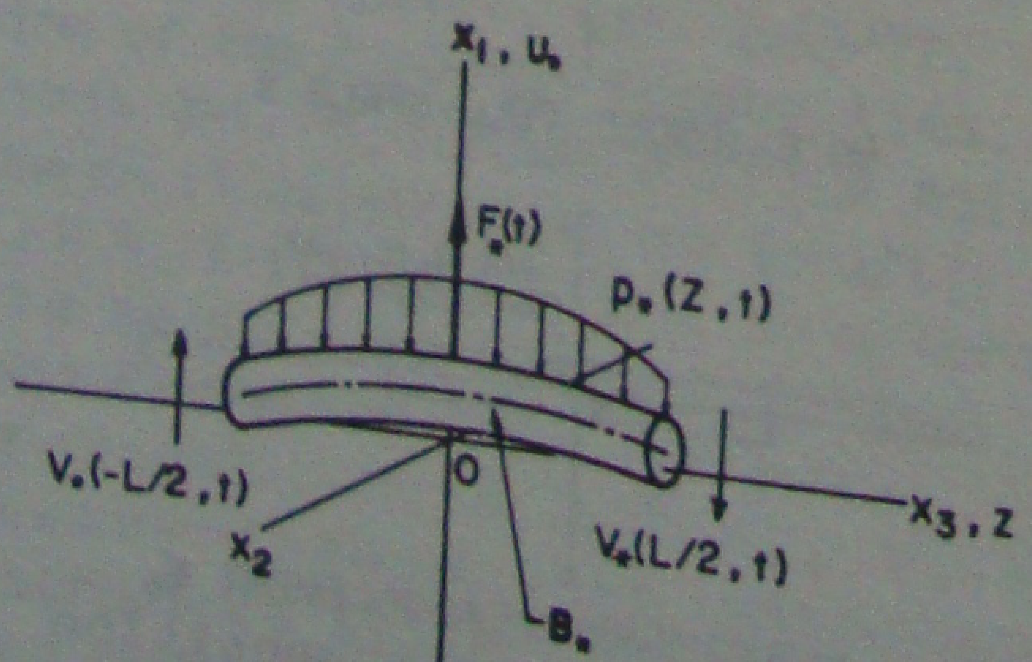

Figure 4: Forces acting on B_*

allow for the possibility of direct load-transfers such as those indicated in (ii) and (iii) in order to maintain a consistent formulation has been discussed in detail in Muki and Sternberg (1968) and will not be repeated here.

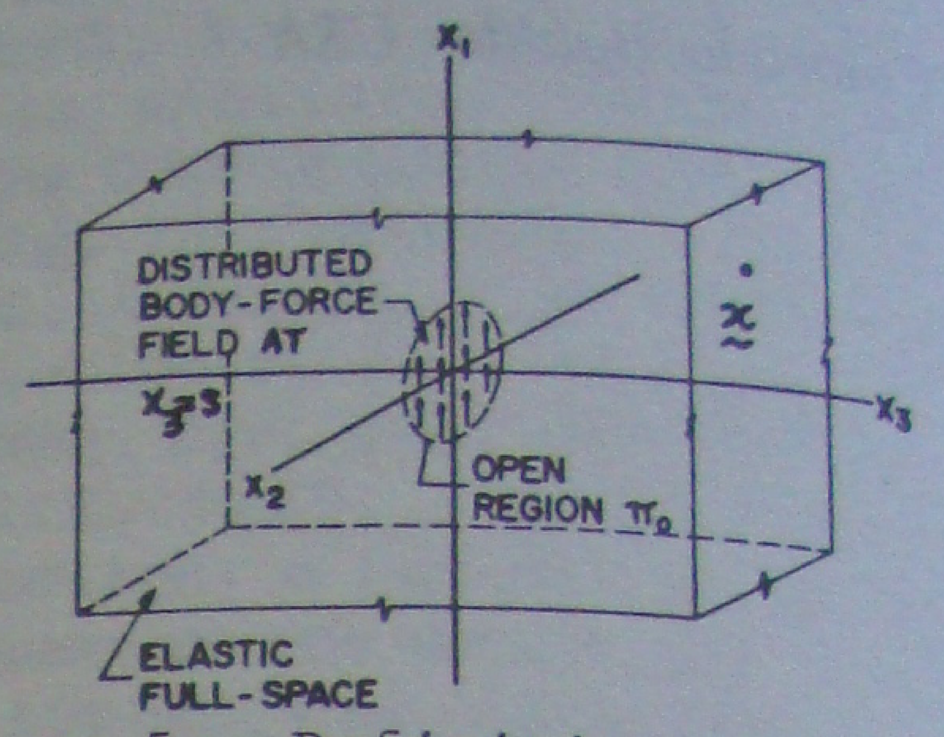

Figure 5: Definition of influence function $\hat{\underline{u}}(\underline{x},s)$

By the law of action and reaction, forces that are equal and opposite to those in (i) and (ii) will be acting on S, in addition to the direct load-transfer of $(F_0 - F_*)$ that occurs at z=0. For the description of the response of the extended medium to the above forces, it is convenient to first determine an influence function $\hat{\underline{u}}(\underline{x},s)$ which gives the displacement field in an elastic full-space due to a time-harmonic body-force field of unit resultant which acts in the x_1-direction. For this analysis, the body-force field is taken to be uniformly distributed over a disk Π_0 which corresponds to the cross-sectional region of the rod (see Figure 5) . With the aid of the influence field, the response of the extended full-space to the interaction forces can be expressed as

$$\underline{u}(\underline{x}) = V_*(L/2)\,\hat{\underline{u}}(\underline{x}, L/2) - V_*(-L/2)\,\hat{\underline{u}}(\underline{x}, -L/2) + (F_0 - F_*)\,\hat{\underline{u}}(\underline{x},0) + \int_{-L/2}^{L/2} p_*(s)\,\hat{\underline{u}}(\underline{x},s)\,ds \quad , \quad x \in S. \qquad (4)$$

To ensure the motion of B_* and S are compatible, a suitable bond condition must be imposed. To this end, the requirement is adopted that the displacement u_* of B_* be equal to u_1 of the medium S along the x_3-axis for the full length of the anchor, i.e.,

$$u_*(z) = u_1(0,0,z) \quad \text{for } -L/2 \le z \le L/2. \qquad (5)$$

On the basis of (4), the above condition can be written as

$$u_*(z) = V_*(L/2)\, \hat{u}_1(z, L/2) - V_*(-L/2)\, \hat{u}_1(z, -L/2) + (F - F_*)\, \hat{u}_1(z, 0) + \int_{-L/2}^{L/2} p_*(s)\, \hat{u}_1(z,s)\,ds \,,$$

$$\text{for } -L/2 \le z \le L/2 \,. \qquad (6)$$

Equation (6) represents the primary governing equation for the soil-structure interaction problem.

2.1 REDUCTION TO A FREDHOLM INTEGRAL EQUATION

With the aids of equations (2) and (3), equation (6) can be shown, through integration by parts, to be expressible as

$$u_*(z) = F_0 \hat{u}_1(z,o) + M_*(z) \left[\frac{\partial \hat{u}_1}{\partial s}(z,s)\right]_{z-}^{z+} + \int_{-L/2}^{L/2} M_*(s) \frac{\partial^2 \hat{u}_1}{\partial s^2}(z,s)\,ds + \omega^2 \rho_* A \int_{-L/2}^{L/2} u_*(s)\, \hat{u}_1(z,s)\,ds \qquad (7)$$

In view of the symmetry of the problem about the x_1-x_2 plane, one may restrict attention to only one half of B_*, i.e., $o \le z \le L/2$. Accordingly, equation (7) can be rewritten as

$$u_*(z) = \frac{F_0}{2} \tilde{u}_1(z,o) + M_*(z) \left[\frac{\partial \tilde{u}_1}{\partial s}(z,s)\right]_{z-}^{z+} + \int_{-L/2}^{L/2} M_*(s) \frac{\partial^2 \tilde{u}_1}{\partial s^2}(z,s)\,ds + \omega^2 \rho_* A \int_{0}^{L/2} u_*(s)\, \hat{u}_1(z,s)\,ds \qquad (8)$$

where $\tilde{u}(z,s) = \hat{u}_1(z,s) + \hat{u}_1(z,-s)$.

By virtue of the representation of u_* in terms of M_* through

$$u_*(z) = \int_0^{L/2} g(z,s)\, M_*(s)\, ds + u_*(L/2), \qquad (9)$$

where

$$g(z,s) = \frac{1}{E_* I} \begin{cases} L/2 - s \,, & z < s \\ L/2 - z \,, & z > s \end{cases} ,$$

one may eliminate the unknown $u_*(z)$ and thus reduces the governing equation to its final form. In dimensionless form, the resulting equation for the problem can be expressed as

$$A(\bar{z})\bar{M}(\bar{z}) - C(\bar{z})\, u(\bar{L}/2) + \int_0^{\bar{L}/2} K(\bar{z},\bar{s})\, \bar{M}(\bar{s})\,d\bar{s} = \bar{F}(\bar{z}) \qquad (10)$$

where

$$A(z) = \left[\frac{\partial U}{\partial \bar{s}}(\bar{z},\bar{s})\right]_{\bar{z}-}^{\bar{z}+} ,$$

$$C(z) = 1 - \frac{\bar{\omega}^2}{4} RM \int_0^{\bar{L}/2} U(z,s)\,ds \,,$$

$$G(\bar{z},\bar{s}) = \begin{cases} \bar{L}/2 - \bar{s} \,, & \bar{z} < \bar{s} \\ \bar{L}/2 - \bar{z} \,, & \bar{z} > \bar{s} \end{cases} , \qquad (11)$$

$$K(\bar{z},\bar{s}) = \frac{\partial^2 U}{\partial \bar{s}^2}(\bar{z},\bar{s}) - RS \left[G(\bar{z},\bar{s}) + \frac{\bar{\omega}^2}{4} RM \int_0^{\bar{L}/2} G(\bar{\eta},\bar{s}) U(\bar{z},\bar{\eta})\,d\bar{\eta}\right] ,$$

$$\bar{F}(\bar{z}) = -\frac{\bar{F}_0}{2} U(\bar{z},o)$$

$$\bar{z} = z/a; \quad \bar{s} = s/a; \quad \bar{L} = L/a, \quad \bar{u} = u_*/a,$$

$$\bar{M} = \frac{M_*}{4\pi\mu_s a^3}, \quad \bar{F} = \frac{F_0}{4\pi\mu_s a^2}, \quad RS = \frac{E_s}{E_*}, \quad RM = \frac{\rho_*}{\rho_s},$$

$$U(\bar{z},\bar{s}) = \frac{2\pi E_s}{(1+\nu_s)} \tilde{u}(z,s)\, ; \quad \bar{\omega} = \omega a / C_s .$$

Here, μ_s, ν_s and C_s are the shear modulus, the Poisson's ratio, and the shear wave speed of the embedding medium, respectively; RS and RM are functions of the modulus ratio $\bar{E} = E_r/E_s$ and the mass ratio $\bar{\rho} = \rho_r/\rho_s$. Equation (10) is a Fredholm integral equation of the second kind, the solution of which furnishes the bending moment profile $\bar{M}(\bar{z})$ and the displacement $\bar{u}(\bar{L}/2)$ of B_*.

3 INFLUENCE FUNCTION

For the solution of equation (10), it is a prerequisite to first obtain the influence function $\hat{u}_1(z,s)$. Using the method of potentials described in Pak (1987), one can show that the influence function $\hat{u}_1$ is given by

$$\hat{u}_1(z,s) = \frac{1}{4\pi\mu_s a}\left(I_1(d) - I_2(d) + 2\, I_3(d)\right)$$

where

$$I_1(d) = \int_0^\infty \frac{\xi^2}{(\xi^2-k^2)^{1/2}} e^{-\bar{\omega}(\xi^2-k^2)^{1/2}d} J_1(\bar{\omega}\,\xi)d\xi\ , \tag{12}$$

$$I_2(d) = \int_0^\infty \frac{\xi^2}{(\xi^2-1)^{1/2}} e^{-\bar{\omega}(\xi^2-1)^{1/2}d} J_1(\bar{\omega}\,\xi)d\xi\ ,$$

$$I_3(d) = \int_0^\infty \frac{1}{(\xi^2-1)^{1/2}} e^{-\bar{\omega}(\xi^2-1)^{1/2}d} J_1(\bar{\omega}\,\xi)d\xi\ ,$$

$$d = \left|z-s\right| \quad , \quad k = \sqrt{\frac{(1-2\nu_s)}{2(1-\nu_s)}} \quad .$$

The above integrals can be evaluated in closed form:

$$I_1(d) = -i\sqrt{\frac{\pi}{2}}\, k^{3/2}\, \bar{\omega}^{-1/2}(d^2+1)^{-3/4}H^{(2)}_{3/2}[k\,\bar{\omega}(d^2+1)^{1/2}]\ ; \tag{13}$$

$$I_2(d) = -i\sqrt{\frac{\pi}{2}}\, \bar{\omega}^{-1/2}(d^2+1)^{-3/4}H^{(2)}_{3/2}[\bar{\omega}(d^2+1)^{1/2}]\ ;$$

$$I_3(d) = -i\,\frac{\pi}{2}\, J_{1/2}[\frac{\bar{\omega}}{2}\,((d^2+1)^{1/2}-d)]\, H^{(2)}_{1/2}[\frac{\bar{\omega}}{2}((d^2+1)^{1/2} \mp d)]$$

In (12) and (13), J_ν is the Bessel function of the first kind of order ν and $H^{(2)}_\nu$ is the Hankel function of the second kind of order ν. Since the Bessel and Hankel functions above are all of fractional orders, they can be expressed in terms of elementary circular functions. This is clearly desirable in the numerical solution of the integral equation as its kernel function and other coefficients can be computed accurately with minimal effort.

4 ILLUSTRATIVE RESULTS AND DISCUSSIONS

To obtain a numerical solution to the governing Fredholm integral equation of the second kind, a variety of techniques exists that will convert the equation into a set of linear algebraic equations which can then be solved on a digital computer. Since the influence function and thus the various coefficients of the integral equation can be computed with great economy and accuracy, the use of a simple method such as quadrature with finer discretization is preferred to more sophisticated schemes which may allow coarser spacings to achieve the same level of accuracy. To this end, a computer code is developed for the solution of the integral equation on the basis of the trapezoidal rule with variable spacings.

With the aid of the computer code, the solution to the soil-structure interaction problem can be computed and selected results are presented in Figures (6) to (8) to illustrate the basic characteristics of the solution. Since the response is in general out-of-phase with respect to the excitation, the response quantities are represented in complex notation, with the real and the imaginary parts denoting the in-phase and the 90 deg out-of-phase components, respectively. From Figure 6, it can be easily seen that the maximum moment always occurs at the point of loading. As expected, the displacement at the point of load application increases while the bending moment decreases as the modulus rato $\bar{E} = E_r/E_s$ decreases. The variation of the response $\bar{u}$ at z=0, commonly called the compliance of the anchor system, as a function of the dimensionless frequency $\bar{\omega}$ is illustrated in Figure 8. As is evident from the figure, there is a strong dependence of the system response on excitation frequency. With the exception of some quantitative differences, the behaviors of the solution at different Poisson's ratio ν_s, mass ratio $\bar{\rho}$, and lengths are similar and hence, for the sake of brevity, will not be pursued here.

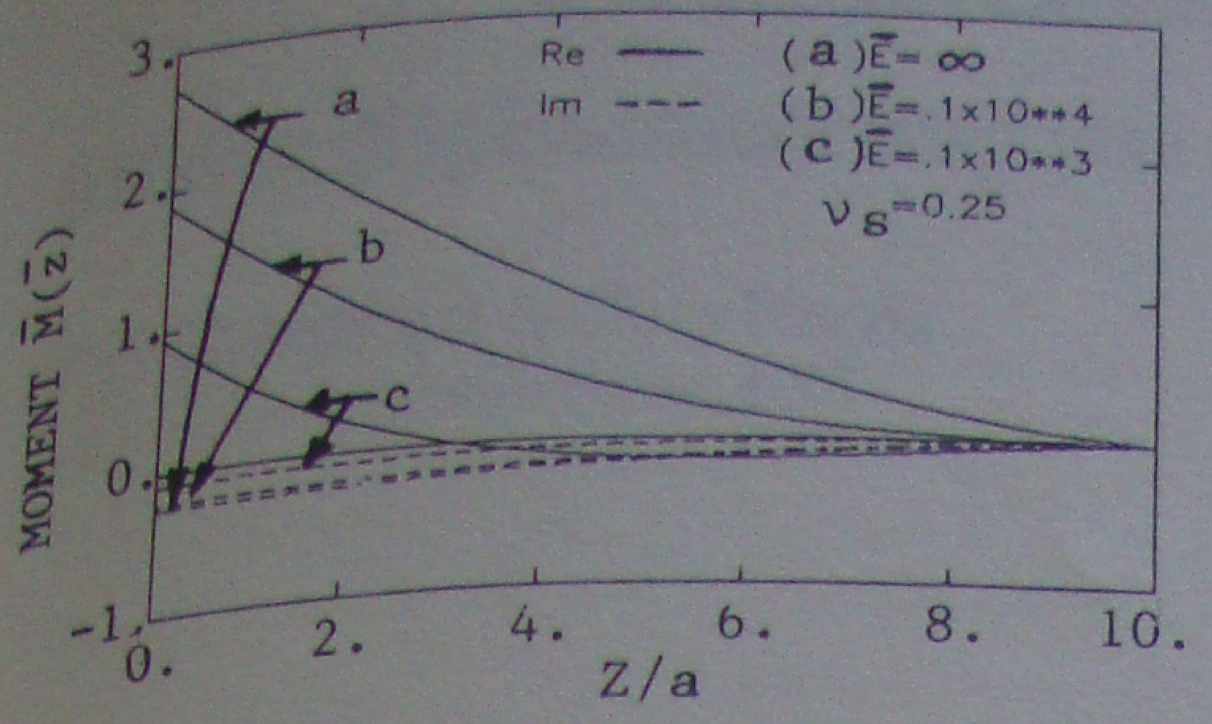

Figure 6: Bending Moment Profile $\bar{\omega}$= 0.3, L= 20a

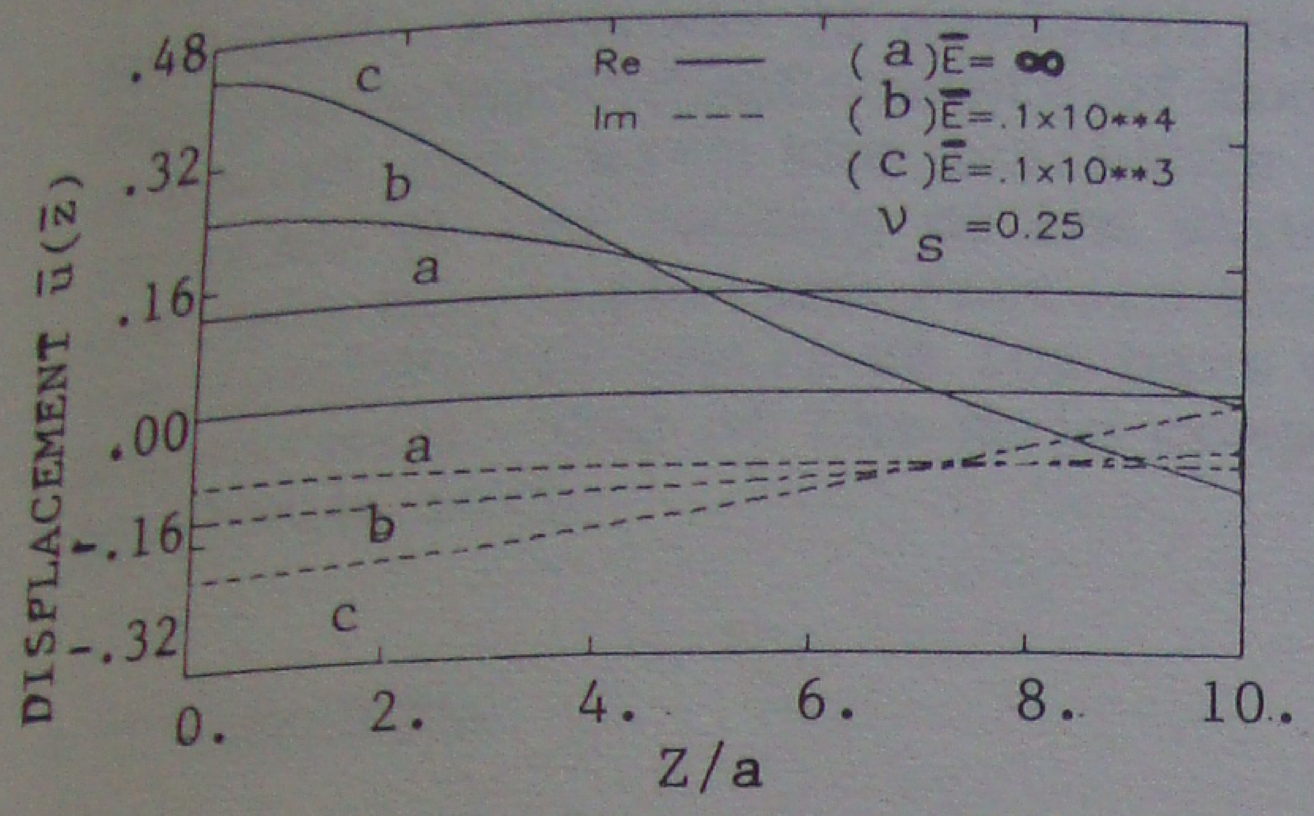

Figure 7: Displacement Profile $\bar{\omega}$= 0.3, L= 20a

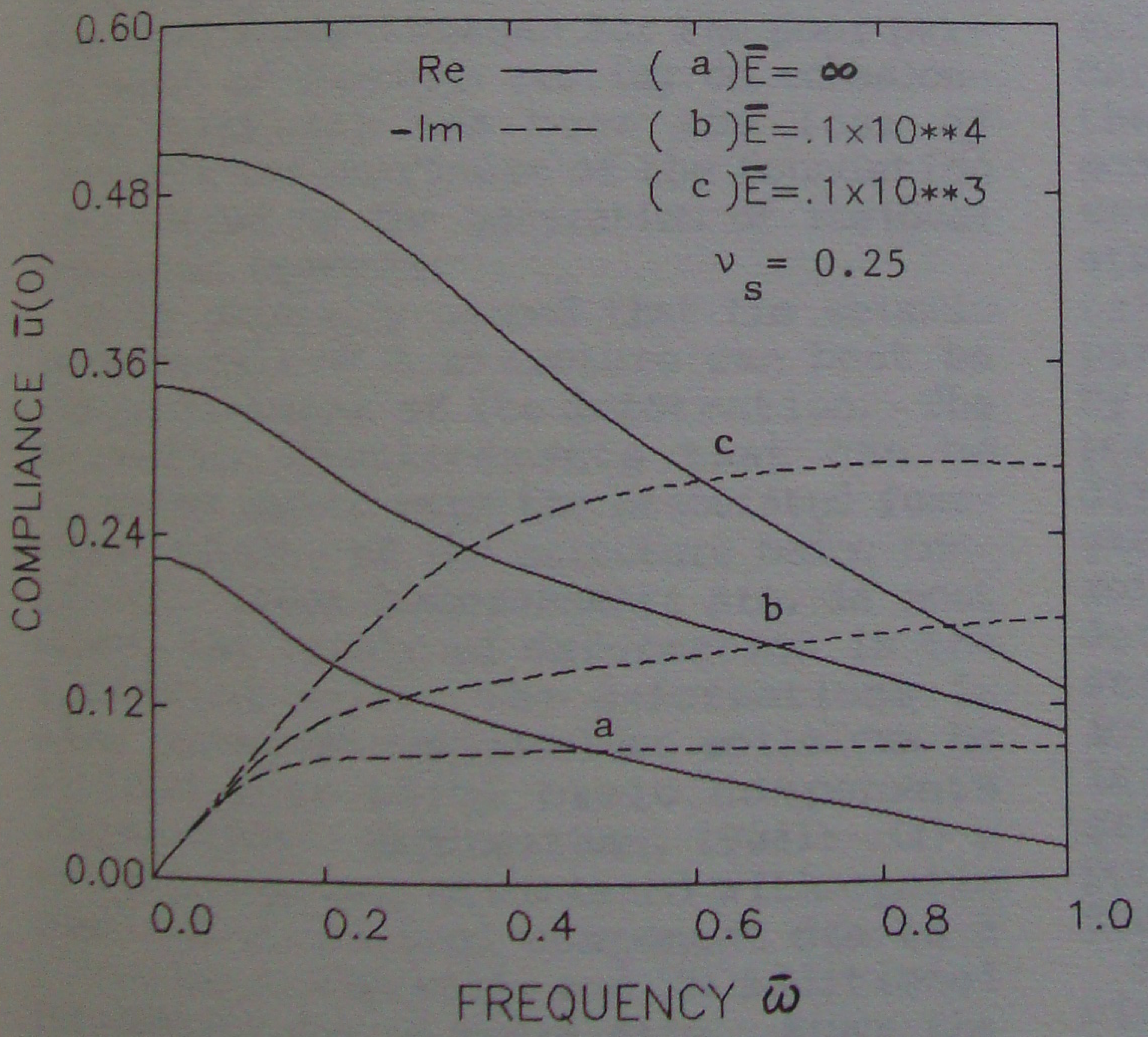

Figure 8: Dynamic Compliance of Anchor Rod System (L=20a) for Unit $\bar{F}$

5 SUMMARY

A formulation is presented for the derivation of the dynamic compliance of a deeply buried anchor rod. In addition to providing a solution of use in soil-structure interaction analysis, it is hopeful that the development presented in this paper suggests a viable formulation for a consistent analysis of lineal buried structures such as piles and tunnels under dynamic earthquake excitations.

6 REFERENCES

Muki, R. and Sternberg, E., 1968. On the diffusion of load from a transverse tension bar into a semi-infinite elastic sheet," J. Appl. Mech., ASME, 35: 737-746.

Muki, R. and Sternberg, E., 1969. On the Diffusion of an Axial Load from an Infinite Cylindrical Bar embedded in an Elastic Medium," Int. J. Solids & Struct.,5: 587-605

Pak, R.Y.S., 1987. "Asymmetric Wave Propagation in an Elastic Half-Space by a Method of Potentials," (in press) J. Appl. Mech., ASME.